Pergamon

Cement and Concrete Research, Vol. 26, No. 3, pp. 363-376, 1996

0008-8846/96 $15.00 + .00

PII S0008-8846(96)00013-0

FIBRE REINFORCED CONCRETE BEAMS UNDER IMPACT LOADING

Nianzhi Wang[1], Sidney Mindess[1] and Keith Ko[2]
[1]Dept. of Civil Engineering, University of British Columbia, Vancouver, B. C. Canada V6T 1Z4
[2]Templeton Senior Secondary School, Vancouver, B. C. Canada

(Refereed)
(Received September 27, 1995; in final form January 3, 1996)

ABSTRACT

Impact tests were carried out on small concrete beams reinforced with different volumes of both polypropylene and steel fibres. The drop height of the instrumented drop-weight impact machine was so chosen that some specimens failed completely under a single drop of the hammer, while others required two blows to bring about complete failure. It was found that, at volume fractions less than 0.5%, polypropylene fibres gave only a modest increase in fracture energy. Steel fibres could bring about much greater increases in fracture energy, with a transition in failure modes occurring between steel fibre volumes of 0.5% and 0.75%. Below 0.5%, fibre breaking was the primary failure mechanism and the increase in fracture energy was also modest; above 0.75% fibre pull-out was the primary mechanism with a large increase in fracture energy.

Introduction

The behaviour of steel fibre reinforced concrete (SFRC) beams under impact loading has been studied extensively (1–5). One of the benefits of SFRC is that its impact resistance, or dynamic toughness, is significantly higher than that of plain concrete. Banthia (6), however, has expressed the concern that, for SFRC, the improvements in the peak load and the fracture energy under impact loading may be considerably smaller than those obtained under static loading. For instance, the addition of 1.5% by volume of steel fibres increased the static peak bending load and fracture energy by factors of 1.81 and 8.14, respectively, compared to the values for the plain matrix. However, under impact loading, the factors were only 1.42 and 2.63, respectively (7). Banthia (6) further suggested that, in order to redesign steel fibres so that they would perform better under impact, we would have to increase our understanding of the pull-out process for deformed fibres.

A technique for testing concrete beams using instrumented drop-weight impact machines was developed at the University of British Columbia by Banthia and his colleagues (1–3,8). These machines have been used for plain concrete, fibre reinforced concrete, and conventionally reinforced and prestressed concrete beams. In the work previously reported, the drop height was chosen so that the specimens failed under a single blow. However, cumulative impact tests (i.e., tests in which failure occurs after a repeated series of impacts, each too small to cause failure

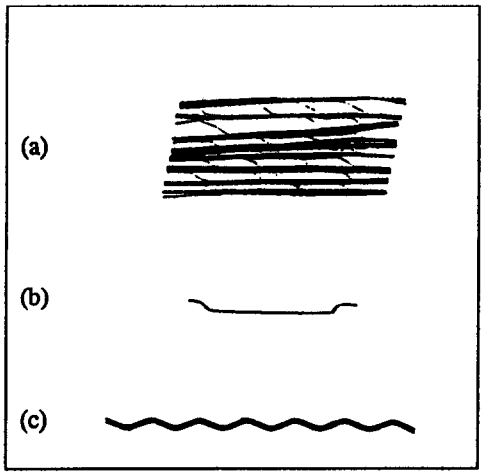

FIG. 1.
Three types of fibres: (a) fibrillated polypropylene; (b) hooked-end steel; (c) crimped steel.

individually) may be needed to simulate certain types of dynamic loading. In practice, some structural members are required to resist repeated impacts, such as concrete railroad ties, airport runways, beam-column joints under earthquake loading, and so on. A "multiple-blow" impact test can better simulate these cases, in terms of both pulse duration and amplitude, and can also take into account the deterioration of the member. Moreover, the total fracture energy of a beam under repeated impact loading is likely to be different from that obtained in a "single blow" test.

In the present study, the original single-blow impact technique has been extended to the case of cumulative impacts, in which some of the beams were not broken at the first blow. Three types of fibres (Fig. 1) were used: 38 mm long fibrillated polypropylene fibres*, 30 mm long hooked-end steel fibres**, and 50 mm long crimped steel fibres***. The effects of these different fibres on the impact behaviour of FRC beams were examined.

Experimental Procedures

Impact Machine. An instrumented drop-weight machine with an impact hammer weighing 60.3 kg was used. For these tests, the drop height was held at 150 mm throughout. A load cell installed in the hammer tup was used to record the impact loads. An accelerometer was fastened to the bottom of the beam at mid-span. The data from the load cell and the accelerometer were collected at 10 μs intervals using a PC based data acquisition system. A more detailed description of this impact machine has been given elsewhere (9). A schematic sketch of the test setup is shown in Fig. 2.

*Forta Corporation, USA
**NV Bekaert SA, Belgium
***Eurosteel SA, Belgium

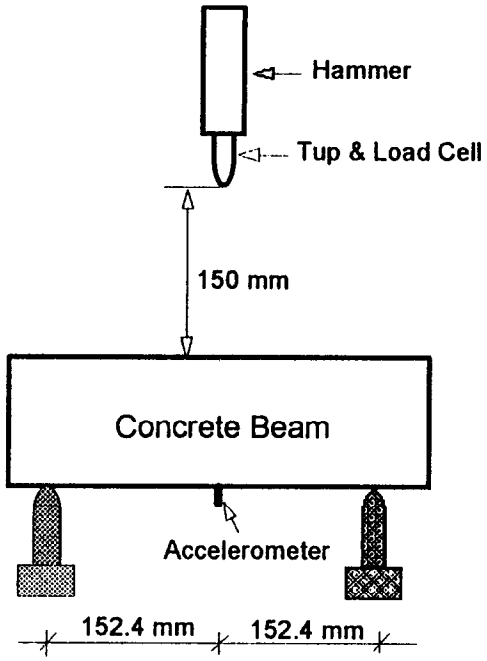

FIG. 2.
Impact test setup.

FRC Specimens. The FRC specimens were cast in 102.4 × 102.4 × 355.6 mm molds. The basic matrix mix design was 1.0:0.4:2.4:2.2 (cement : water : fine aggregate : coarse aggregate), with a maximum aggregate size of 10 mm. A superplasticizer was used to provide reasonable workability. The specimens were demolded at one day, and were then cured in water and tested at an age of 14 days.

Nine different types of FRC were produced; three specimens of each type were tested on a 304.8 mm span, simply supported. The specimen types are described in Table 1.

Method of Analysis. The method of analysis developed previously (1,8) was used for analyzing those FRC beams which failed completely at the first blow. For those beams which did not fail under the first blow, however, the method of analysis had to be modified. In the following, the original method is introduced briefly, and then the modifications made for the present study are described.

1) If the system can be approximated by a single degree of freedom model, and the damping of the beam can be neglected, then the equation of dynamic equilibrium is

$$M\ddot{u}(t) + P_b(t) = P_t(t) \tag{1}$$

where M is the generalized mass of the beam, P_t is the tup load, P_b is the true bending load and $\ddot{u}$ is the mid-span acceleration of the beam. $M\ddot{u}\ (t)$ may be referred to as the inertial load, P_i. Then, the true bending load is

TABLE 1

Specimen Types

Specimen ID	Fibres Used
N	No fibres
p1	0.25% polypropylene fibres, 38 mm
p2	0.50% polypropylene fibres, 38 mm
s1	0.25% hooked steel fibres, ϕ0.5 × 30 mm
s2	0.50% hooked steel fibres, ϕ0.5 × 30 mm
s3	0.75% hooked steel fibres, ϕ0.5 × 30 mm
s4	1.00% hooked steel fibres, ϕ0.5 × 30 mm
s5	1.50% hooked steel fibres, ϕ0.5 × 30 mm
w	0.75% crimped steel fibres, ϕ1.0 × 50 mm

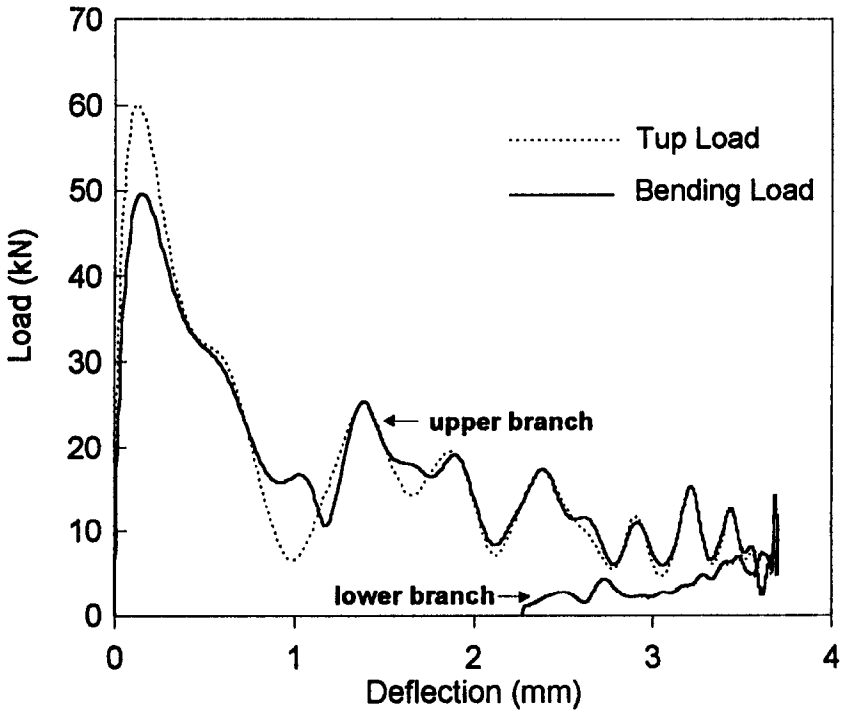

FIG. 3.
Load vs. deflection curve for S3-2 (0.75% steel fibres).

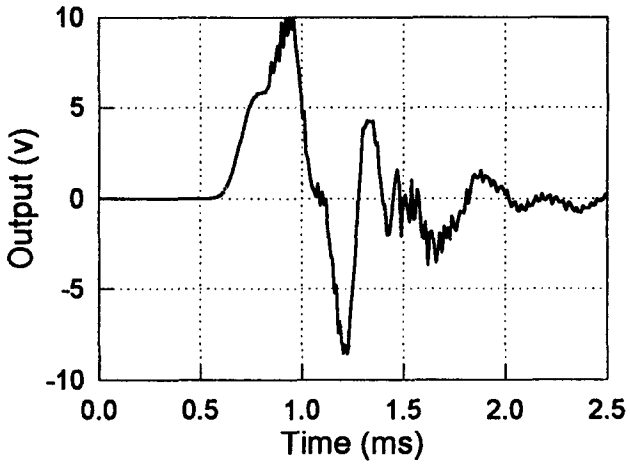

FIG. 4.
Original signals of the accelerometer.

$$P_b = P_t - P_i \tag{2}$$

When the specimen is broken by a single blow, the measured accelerations, and hence P_i, are always positive. Thus, the bending load P_b is always less than the tup load, P_t. However, when the beam does not fail completely under a single blow, it must undergo first an acceleration, and then a deceleration before it finally comes to rest. During the deceleration, $\ddot{u}$ is negative, and hence so is P_i. Thus, P_b will be greater than P_i during this period. Fig. 3 shows a typical example with both tup load and true bending load vs. deflection curves for a beam which was not broken at the first blow.

Similarly, if the beam is broken by a single impact, the flexural energy absorbed by the beam (defined as the area under the complete load vs. deflection curve) is less than the total energy lost by the hammer during its fall. The difference between the total energy lost and the flexural energy absorbed represents the sum of the inertial energy and the kinetic energy of the broken pieces of the beam. However, if the beam is not broken into two or more pieces, the flexural energy absorbed should be very close to the energy released by the hammer. That is, the areas under the bending load versus deflection curve and the tup load versus deflection curve should be similar. This is because the inertial and kinetic energies transferred to the beam while it was being accelerated were gradually released back to the system as the beam returned to rest. No energy transferred from the hammer to the beam, via the tup load, was lost.

2) Since the beam remains intact (though damaged), it must retain some elasticity; that is, after the beam reaches its maximum deflection, it springs back to some extent. During this time, the beam velocity at mid-span, $\dot{u}$ (obtained by the integration of the acceleration $\ddot{u}$) is negative, and the deflection u (obtained by the integration of the velocity $\dot{u}$) decreases from its maximum value. Figure 2 shows a typical example. Note that the bending load did not fall to zero, since the beam and the hammer maintained contact as the beam rebounded. Thus, the flexural energy consumed by the damage to the beam should be the difference between the area under the upper branch of the bending load versus deflection curve (representing the downward deflection of

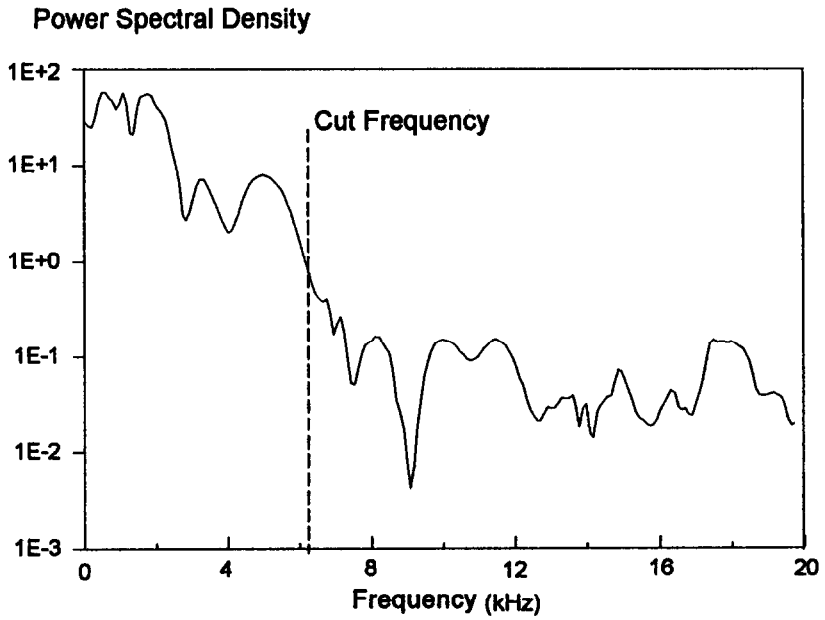

FIG. 5.
Power spectrum of acceleration.

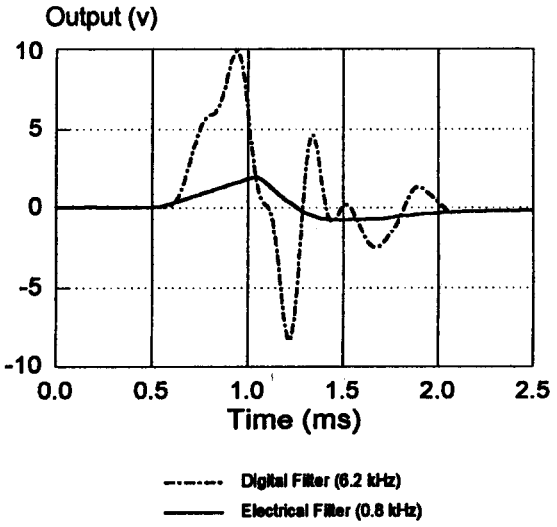

FIG. 6.
Filtered acceleration signals using different filters.

the beam) and the area under the lower branch of the curve (which represents the rebound of the beam), as shown in Fig. 3.

3) In previous studies (1–3,8), low-pass electrical filters (800 Hz) had been used to filter the noise in the data acquisition system, which worked well when the load impulse was relatively long (about 3 ms or more). However, in the present study, the length of time required to reach the peak load (the rise time) was typically only 0.3 to 0.4 ms, which would be less than the rise time of the data acquisition system with the filter (about 0.5 ms). Thus, in the present tests, no filters were used in the data acquisition system. An example of the original data for an acceleration record is shown in Fig. 4. Instead, the data were filtered digitally using the PC computer software MATLAB*. The data were first transformed from the time domain into the frequency domain, as shown in Fig. 5. In this figure, it may be seen that the frequencies of the major vibration modes were concentrated in the range 0–6200 Hz. Higher frequencies were considered to be noise, and so the cut-off frequency was set at 6200 Hz. The low pass digital filtering process was then carried out using this cut-off frequency. Fig. 6 compares the data obtained with an electrical filter to that obtained using the digital filtering described above. The two signals are very different, in that the peak load was greatly reduced by the electrical filter, and there was a considerable delay before the signal reached its maximum.

Results and Discussion

The detailed test results for all of the specimens tested are given in Table 2. In this table, "total work done" is represented by the entire area under the tup load vs. deflection curve; "fracture energy" is represented by the area under the bending load vs. deflection curve. When the beam is not broken by a particular impact, almost all the work done by the falling hammer is transferred into fracture energy. However, when the beam is broken into two or more pieces by an impact, part of the work done by the beam is transferred into kinetic energy of the broken pieces. In this case, the energy consumed in the fracture process itself is less than the work done by the falling hammer. The plain concrete specimens, the polypropylene fire specimens, and the steel fibre specimens for fibre contents up to 0.5% by volume all broke completely under the first blow. However, specimens reinforced with 0.75% or more of hooked steel fibres required two blows to cause the beams to break completely; and one specimen with 0.75% crimped steel fibres required three blows (specimen ID's with an "s" or "t" as the last symbol in Table 2). The given deflections were all obtained from integration of the acceleration records

Fig. 7 shows the fracture energies for the different concretes tested. The values represent the average of the two or three specimens tested of each type.

1. Polypropylene Fibres. Adding polypropylene fibres to the beams did not bring about much improvement in the fracture energies, compared to the unreinforced matrix. Even at 0.50% polypropylene fibres by volume, the increase was only about 21%. Figure 8 shows typical load versus deflection curves for the polypropylene fibre beams. The maximum loads are essentially the same as those for the plain concrete matrix; somewhat larger deflections caused the higher fracture energies. This suggests that, in dynamic loading situations, the "bridging" effect of these fibres is not very significant.

*Developed by The MathWorks, Inc., Version 3.5 m, 1992

TABLE 2

Summary of Impact Tests of FRC Beams

Specimen ID	Maximum Tup Load (kN)	Maximum Bending Load (kN)	Total Deflection (mm)	Total Work Done (N*m)	Fracture Energy (N*m)
N-1	66.7	47.2	0.52	17.8	11.8
N-2	83.2	56.9	0.44	19.6	12.0
N-4	74.5	49.5	0.41	19.9	12.9
Average:	**74.8**	**51.2**	**0.46**	**19.1**	**12.2**
P1-1	69.2	53.0	0.48	21.1	14.3
P1-3	71.2	51.6	0.47	20.5	13.0
P1-4	75.1	52.6	0.63	22.4	15.7
Average:	**71.8**	**52.4**	**0.52**	**21.3**	**14.3**
P2-1	60.0	45.6	0.66	20.0	15.6
P2-3	49.3	39.4	0.63	17.3	12.9
P2-4	64.7	50.1	0.66	21.4	16.1
Average:	**58.0**	**45.1**	**0.65**	**19.6**	**14.9**
S1-1	61.9	39.9	0.79	16.4	10.4
S1-2	52.1	40.7	0.80	19.8	17.6
S1-4	44.8	37.8	0.79	22.5	18.6
Average:	**52.9**	**39.5**	**0.79**	**19.6**	**15.5**
S2-2	64.7	51.5	0.89	24.6	19.5
S2-3	56.3	43.3	0.78	22.7	17.0
S2-4	83.5	59.1	0.48	21.0	15.1
Average:	**68.2**	**51.3**	**0.72**	**22.8**	**17.2**
S3-2	60.5	50.0	3.70	66.0	66.0
S3-2s	38.7	21.8	0.40	6.7	3.4
S3-2 Total:	—	—	4.10	72.7	69.4
S3-3	62.7	48.1	5.96	71.2	71.2
S3-3s	47.1	27.7	0.52	6.0	2.1
S3-3 Total:	—	—	6.48	77.2	73.3
Average:	**61.6**	**49.0**	**5.29**	**74.9**	**71.3**
S4-1	75.9	56.1	2.18	70.9	70.9
S4-1s	77.4	32.9	0.50	17.8	9.8
S4-1 Total:	—	—	2.68	88.7	80.7
S4-3	65.3	50.7	3.8	63.2	63.2
S4-3s	50.7	21.4	0.33	8.3	2.6
S4-3 Total:	—	—	4.14	71.5	65.8
S4-4	69.2	52.2	4.47	68.4	68.4
S4-4s	49.0	26.6	1.00	19.9	11.9
S4-4 Total:	—	—	5.47	88.3	80.2
Average:	**70.1**	**53.0**	**4.10**	**82.8**	**75.6**

(Continued)

TABLE 2
(Continued)

Specimen ID	Maximum Tup Load (kN)	Maximum Bending Load (kN)	Total Deflection (mm)	Total Work Done (N*m)	Fracture Energy (N*m)
S5-2	78.7	62.0	3.63	72.3	72.1
S5-2s	67.5	32.1	1.00	19.4	10.6
S5-2 Total:	—	—	4.62	91.8	82.8
S5-3	60.7	54.7	2.85	78.4	78.4
S5-3s	64.2	37.0	0.39	13.3	6.7
S5-3 Total:	—	—	3.23	91.6	85.0
Average:	**69.7**	**58.3**	**3.93**	**91.7**	**83.9**
W-1	67.5	51.4	4.13	76.2	75.9
W-1s	33.1	25.6	5.13	47.4	47.4
W-1t	23.0	22.2	0.97	7.0	3.2
W-1 Total:*	—	—	10.23	130.6	126.6
W-2	69.0	50.4	8.31	65.3	61.2
W-3	68.4	52.8	3.64	54.9	45.7
Average:	**68.7**	**51.6**	**5.97**	**60.1**	**74.5**

*An examination of the fracture surface of this beam showed an inordinately high fibre concentration, presumably due to random fluctuations in fibre concentration.

2. Hooked Steel Fibres. Figure 9 shows typical load versus deflection curves for beams with 0.5%, 0.75% and 1.5% by volume of hooked steel fibres. As shown in Fig. 10, the fracture energy of the beams increased with increasing fibre content. However, the fracture energies at 0.25% and 0.5% fibre volumes were not much greater than those for the plain concrete; their

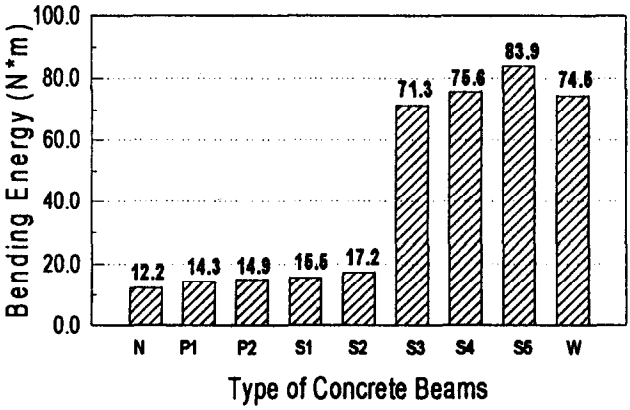

FIG. 7.
Fracture energy of concrete beams with different types of fibres.

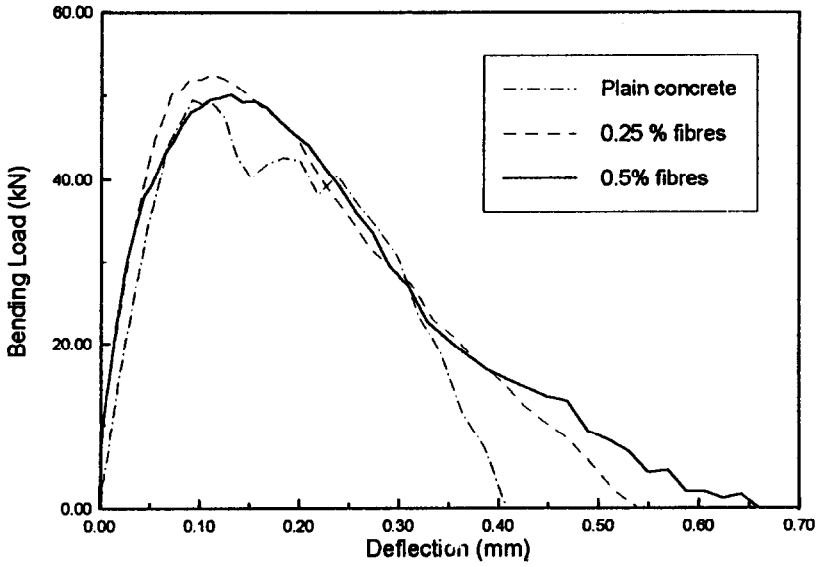

FIG. 8.
Bending load vs. deflection curve for concrete beams with polypropylene fibres.

load vs. deflection curves were very similar. A large jump in fracture energy occurred between 0.5% and 0.75% fibres. Beyond 0.75% fibres, the increases in fracture energy with increasing fibre content were again modest. This suggests an "optimum" fibre content, when expressed in terms of the best property/cost ratio.

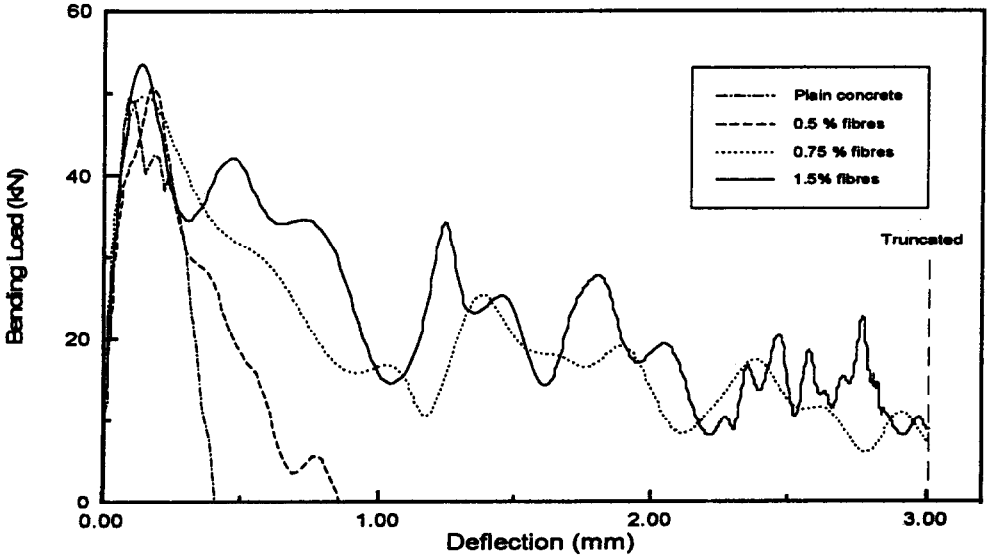

FIG. 9.
Bending load vs. deflection curve for concrete beams with hooked steel fibres.

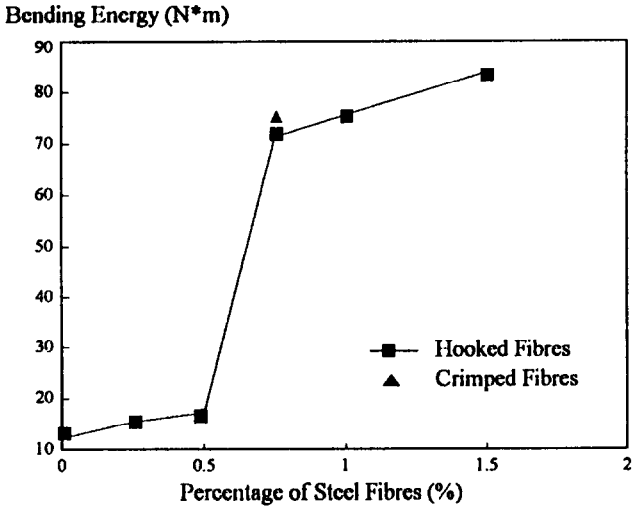

FIG. 10.
Fracture energy of concrete beams with steel fibres.

As shown in Fig. 9, the steel fibres increased the peak bending load only slightly; the major contribution of the steel fibres to the fracture energy lies in the significantly increased maximum beam deflections, which increased from about 0.4 mm for plain concrete to as high as 3 mm for the 1.5% fibre content. Moreover, as stated earlier, beams with 0.75% fibres or more required two blows to bring about failure. They deflected further, and absorbed additional energy when subjected to the second blow (which did cause failure in all cases). In addition, visual examination showed that, for fibre contents of 0.75% or more, the fibres had a much greater tendency to pull out rather than to break. Occasionally, a second flexural crack appeared beside the main flexural crack.

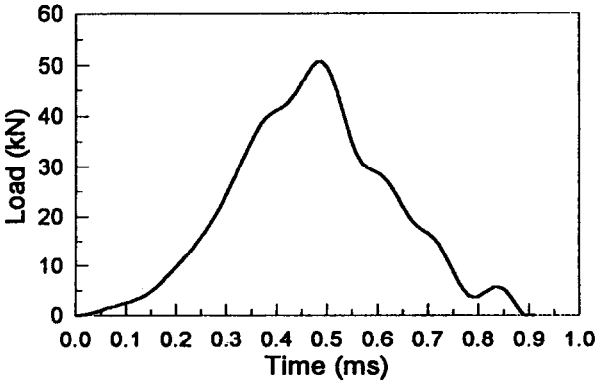

FIG. 11.
Bending load history of the beam with 0.5% fibres.

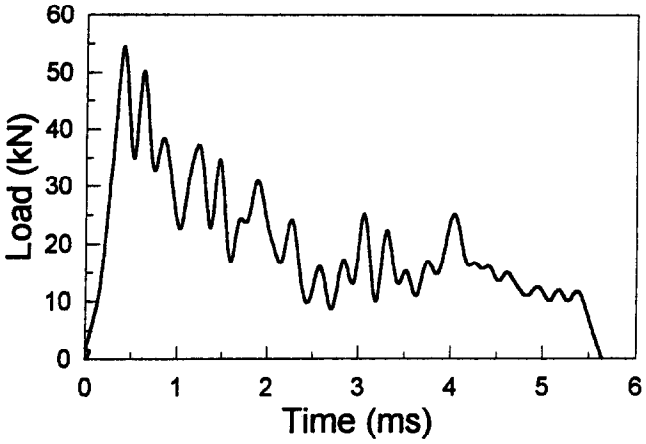

FIG. 12.
Bending load history of the beam with 1.5% fibres.

One possible explanation for the large jump in fracture energies between 0.50% and 0.75% fibres may be the differences in the fracture process. For lower fibre contents, the total failure event lasted about 1 ms (Fig. 11), and the average deflection was about 0.8 mm. The fibres had a greater tendency to break. For higher fibre contents (Fig. 12), the total failure event lasted for more than 5 ms, and the average deflection was 4–5 mm, consistent with a fibre pull-out rather than a fibre breaking mode of failure. At these higher fibre contents, the fibres were able to support sufficient load to necessitate a second blow to cause failure.

Based on the results above, the following mechanism for the fibre failure modes in concrete beams under impact loading may be suggested:

a) The pull-out process of hooked steel fibres must be accompanied by microcracking processes at the interface between the fibres and the matrix. The microcracking needs a higher load to initiate under impact than under static loading due to the stress rate sensitivity of concrete. In other words, a hooked steel fibre has a greater tendency to break rather than to be pulled out under impact loading.

b) When the first crack occurs at the bottom of the beam, only a small amount of tensile stress can be transmitted by the concrete across the crack. The tensile force must be transferred from the concrete to the reinforcing fibres, resulting in a great increase of steel stress in the vicinity of the crack. Since the fibres have a greater tendency to break under impact, they will tend to break immediately ***unless*** the fibre volume is high enough to resist all the tensile force transferred from the concrete at the crack. Similar to reinforced concrete, which needs a minimum percentage of reinforcing steel to prevent the steel from breaking when concrete first cracks (10), the SFRC also needs a minimum percentage of fibres to avoid a fibre breaking failure under impact loading.

3. Crimped Steel Fibres. The beams made with 0.75% by volume crimped steel fibres had similar load vs. deflection curves (Fig. 13) and about the same fracture energies as those made with 0.75% hooked steel fibres, and they too failed primarily in a fibre pull-out mode. This suggests that the effectiveness of these two types of fibres was similar.

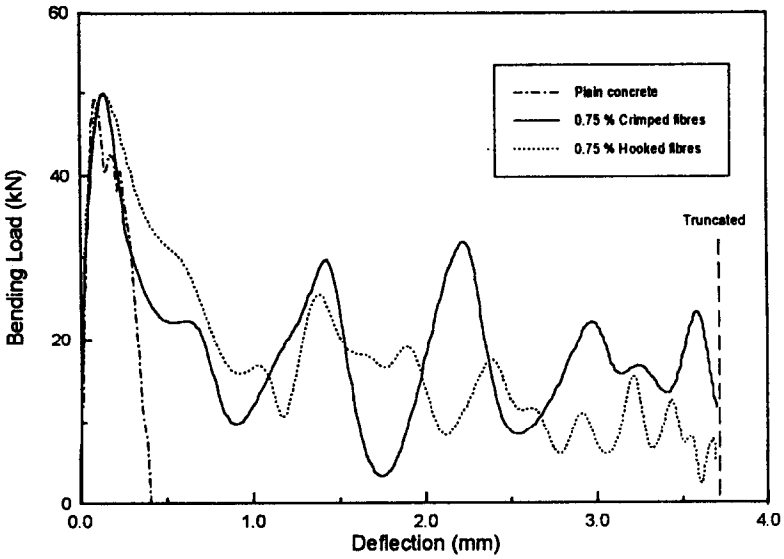

FIG. 13.
Bending load vs. deflection curve for concrete beams with 0.75% crimped steel fibres.

From Table 2, it may be seen that one of the beams with crimped fibres had a very high fracture energy. An examination of the fracture surface showed an inordinately high fibre concentration in the beam, presumably due to random fluctuations in fibre concentration.

4. Implications of the Present Study. The results of this study suggest that, for the design of fibre reinforced concrete elements for a particular severity of impact loading, a critical fibre content exists. For fibre additions below this critical fibre content, the properties of the element will be only little improved. On the other hand, fibre additions much beyond this fibre content will not be very efficient. It appears that, the higher the loading rate, the greater the critical fibre content.

Conclusions

1. An analytic procedure was developed for the impact testing of the beams which were not completely broken at one blow.
2. The addition of fibres to concrete at fibre volumes of up to 0.5% led to only small increases in fracture energy. For 0.5% polypropylene fibres, the increase was about 22%; for 0.5% steel fibres, the increase was about 41%.
3. With an increasing volume of hooked steel fibres, the fracture energy of the beams increased. There appeared to be a critical volume of fibres at which the fracture energy of the beam jumped to a much higher level; beyond this point, there was only a small increase in fracture energy with further increases in the volume of the steel fibres.

4. Two different fracture mechanisms exist in SFRC beams made with hooked fibres. Below the critical volume of fibres, there seems to be a fibre breaking failure mechanism; above the critical fibre volume, there is primarily a fibre "pull-out" mechanism. The critical value for the hooked steel fibres in this series of tests is between 0.5% and 0.75%.

References

1. Banthia, N.P., Impact Resistance of Concrete, Ph.D. Thesis, Department of Civil Engineering, University of British Columbia, Canada, 1987.
2. Banthia, N.P., Mindess, S. and Bentur, A., Materials and Structures, 20, 293, (1987).
3. Banthia, N.P., Mindess, S. and Bentur, A., Proc., Int. Symp. Fibre Reinforced Concrete (ISFRC-87), Madras, 4.29 (1987).
4. Suaris, W. and Shah, S.P., ASCE J. Struct. Div., 109, 1717 (1983).
5. Suaris, W. and Shah, S.P., J. ACI, 83, 117 (1986).
6. Banthia, N.P., Cement and Concrete Science and Technology, p. 288, (Ed.) Ghosh, S.N., AGI Publishers, India.
7. Banthia, N.P., Mindess, S. and Bentur, A., in Proceedings, Sixth International Confrence on Composite Materials, London, July 1987.
8. Banthia, N.P., Mindess, S., Bentur, A. and Pigeon, M., Experimental Mechanics, 29, 63 (1989).
9. Wang, N., Mindess, S. and Venuti, W. J., "Resistance of Concrete Railroad Ties to Impact Loading", to be published on AREA Bulletin.
10. Collins M. P. and Mitchell, D., Prestressed concrete basics, p.149, Canadian Prestressed Concrete Institute (1987).